

FULL ARTICLE

Dermal carotenoid measurements via pressure mediated reflection spectroscopy

Igor V. Ermakov and Werner Gellermann*

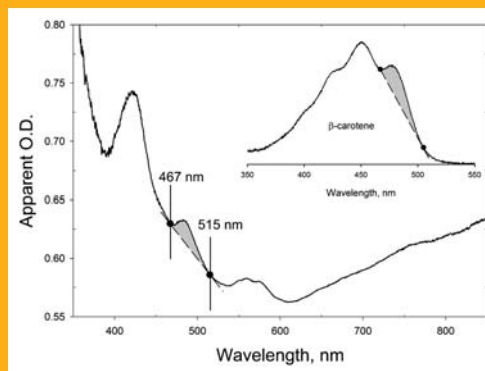
Department of Physics and Astronomy, University of Utah, Salt Lake City, UT 84112, USA

Received 7 November 2011, revised 23 December 2011, accepted 4 January 2012

Published online 10 February 2012

Key words: Reflection spectroscopy, skin, carotenoids, antioxidants

We describe a reflection-based method for the quantitative detection of carotenoid antioxidants in living human skin. The skin tissue site of interest is illuminated with broad-band white light spanning the spectral range from 350–850 nm and the spectral composition of the diffusively reflected light is analyzed in real time. Topical pressure is applied to temporarily squeeze blood out of the illuminated tissue volume. In this way the influence of oxy-hemoglobin on the reflection spectra is effectively reduced. After a short optical clearing time the carotenoid absorption becomes easily discernable in a 460–500 nm spectral window and its optical density can be calculated with high accuracy. Our empirical methodology provides a non-invasive rapid determination of skin carotenoid levels, can be used to monitor skin carotenoid concentration changes over time in response to carotenoid containing natural or supplemental diets, and is easily adaptable for applications in clinical and field settings.



Determination of human skin carotenoid levels from reflection-based absorption spectra. After temporarily squeezing blood out of the measured tissue volume, a carotenoid-related absorption band (shaded area), which is superimposed on a residual scattering background, is discernible in the 467 to 515 nm region. It is due to the one-phonon vibronic absorption transition of carotenoids, shown for comparison also in the insert for a pure β -carotene solution. The optical density of the skin carotenoid one-phonon absorption is used as a quantitative measure for the skin carotenoid levels.

1. Introduction

Carotenoids have widespread distributions in fruits and vegetables. Taken up through the diet, their presence in living human skin can serve as an objective biomarker of fruit and vegetable intake. Fruit and

vegetable consumption is generally regarded as an important factor for increased energy and overall good health. For example, high dietary consumption of fruits and vegetables has been associated with protection against various cancers [1, 2], cardiovascular disease [3], and macular degeneration [4].

* Corresponding author: e-mail: werner@physics.utah.edu, Phone: 801-581-5222, Fax: 801-581-4801

Furthermore, carotenoids themselves have been speculated to be one of the anti-carcinogenic phytochemicals of plant foods [1] and are thought to protect the macula from photo-toxic light through filtering and/or antioxidant action [5]. For all these reasons it is compelling to develop convenient detection methodologies for carotenoids directly in living human tissue.

The assessment of carotenoid status has often relied upon the collection of plasma or serum samples for high-performance liquid chromatography (HPLC) analysis. While considered to be the current standard, this approach has several important limitations, including high cost and fluctuating carotenoid concentrations in blood due to relatively short half-lives. Also, in the human retina, only two of the approximately half a dozen carotenoid species circulating in blood, i.e. lutein and zeaxanthin, are taken up and concentrated in this tissue, which is due to a process controlled by a highly selective protein binding mechanism. As a consequence, there is at best only a poor correlation with plasma levels, and it is necessary to develop non-invasive methods suitable to assess carotenoid status directly in the tissue of interest.

Initially, our group had developed Resonance Raman spectroscopy, RRS, as an objective indicator of carotenoid status in the living human retina and skin [6–10]. This highly molecule specific methodology is based on the Raman response originating from the vibrating carbon backbone that is common to all carotenoids [11]. The backbone's carbon-carbon single-bond and double-bond stretch frequencies each generate a spectrally sharp, resonantly enhanced Raman signal when excited in any of their vibronic absorption transitions in the visible wavelength region. The Raman lines are shifted from the excitation light frequency by exactly the amount of the respective vibrational stretch frequency, i.e. by 1159 and 1525 cm^{-1} , respectively. Since these frequencies are relatively large, they translate into large wavelength shifts of several ten nm when excited in the visible. Superimposed on a large fluorescence background, the Raman lines are readily isolated from the excitation light with a medium resolution (~ 1 nm) spectrograph and their strengths can be easily quantified with a linear detector array if it has a high dynamic range. Choosing an excitation wavelength in the spectral vicinity of 480 nm, RRS measures the combined concentrations of all resonantly excited carotenoids in skin [6, 8, 10], including beta-carotene, lycopene, beta cryptoxanthin, lutein and zeaxanthin, and their isomers. Phytoene and phytofluene, two carotenoids found in skin [18] that have shorter conjugation lengths and corresponding absorptions in the UV, are not detected. In the human retina, RRS can be used to measure the combined concentration of lutein and zeaxanthin in the ~ 1 mm

diameter macular region with spatially integrating instruments [7, 12] or with spatially resolved imaging configurations [13].

One of the preferred body sites for Raman based skin carotenoid measurements has been the palm of the hand [6, 8–10] because the dermal melanin pigment is lighter and less variable among individuals of different racial and ethnic backgrounds. Additionally, the stratum corneum, the outer dermal tissue layer, is relatively thick in the palm (at least ~ 400 μm). This insures that the excitation light does not penetrate beyond this strongly scattering layer (light penetration depth ~ 200 μm) into the deeper tissue layers where it could excite other, potentially confounding chromophores. In first field applications with a portable instrument configuration we could demonstrate the suitability of the RRS methodology for the rapid measurement of large subject populations. Measurements of the palms of 57 subjects produced a bell-shaped distribution [8] with significant width ($\sim 50\%$ of the central value), proving that important characteristics of an objective marker of carotenoid status such as inter-subject variability could be easily reproduced in a non-invasive fashion.

Based on these results, RRS based skin carotenoid detection could be readily developed for commercial applications in the nutritional supplement industry ["Biophotonic Scanner", NuSkin/Pharmanex Inc., Provo, Utah]. In this endeavor, our initial argon-laser based prototype instrument was miniaturized into a field-usable portable RRS instrument, based on a low-power compact 473 nm solid state laser and 65 mm spectrograph/CCD detector combination. At a later stage, a more rugged non-laser version was developed based on spectrally narrowed LED excitation in combination with photomultiplier detection [14]. Presently, about ten thousand portable RRS instruments are in use in the nutritional supplement industry, with the total number of measured subjects reaching about 10 million. Based on these high population numbers, the RRS methodology provides insight with high statistical significance into effects of diets, external stress factors such as smoking, and population differences. Most significantly, it proves the efficacy of carotenoid-containing nutritional supplement formulations in this industry [15, 16].

In comparison, the acceptance of RRS in the scientific and medical arena has been relatively slow, first awaiting a rigorous validation of the concept with HPLC-derived carotenoid levels. Initially we could show that carotenoid levels measured with RRS in the inner palm of the hand correlate strongly and significantly with HPLC-derived carotenoid levels of fasting serum, thus validating the method in an indirect way [16]. More recently, we completed direct validation experiments involving skin carotenoid RRS measurements followed by biopsy of the

measured tissue volume and subsequent HPLC analysis [17, 18]. Again, a high correlation was found between both methods. RRS is now finding increasing use as rapid objective carotenoid biomarker also in areas such as Nutrition [19, 20, 21], Cancer Prevention [22] and Neonatology Research [23].

In this manuscript, we describe an alternative optical method for the non-invasive assessment of skin carotenoids. This method is a variation of reflection spectroscopy, measuring the skin carotenoid absorption via reflection under application of topical pressure [24]. It holds promise as a particularly simple and inexpensive method since it does not require any narrow-band light sources for excitation or relatively high-resolution spectrometers for detection of the spectrally narrow Raman line features.

Reflection spectroscopy has been used previously to quantify carotenoid macular pigments in the human retina [25]. Compared to the skin, however, carotenoid levels in the healthy human macula are about two orders of magnitude higher, and the concentrations of potentially confounding chromophores in the retina are relatively low. Furthermore, the optical media of the human eye anterior to the retina are relatively transparent. Typically, they cause only modest light scattering, and the sclera of the eye can be used as a light reflector that realizes a more or less straight double-path propagation of the excitation light through all ocular tissue layers to the sclera and back. These favorable conditions make it possible to use a multi-layer sequential light transmission model in which the individual absorption and/or scattering effects are described with 8–10 respective absorption and/or scattering coefficients, and in which the macular carotenoid pigment levels are derived from a multi-parameter fit of the calculated reflection spectra to the measured spectra.

In human skin, the much stronger light scattering caused by the outer stratum corneum layer does not permit the assumption of tissue light propagation and modeling of straight light paths. Furthermore, there is no effective internal interface that could be used as a reflector. As a consequence, the methodology of [25] is not applicable. Nevertheless, reflection spectroscopy has been used previously for the measurement of skin carotenoid levels [26, 27]. Attempting to take into account the inhomogeneity of chromophore distributions in the living tissue in this earlier first-principles approach, a complex spectral de-convolution algorithm was used, involving a multi-compartment modeling for skin chromophores. The authors found a significant correlation between baseline skin and serum carotenoid levels in a 12-week β -carotene supplementation study, and they were able to document an apparent rise in response to supplementation in a small group of volunteer subjects [26]. However, the interpretation of reflection spectra within the diffusive light transport mod-

el in turbid media was recognized to be problematic for the assessment of the relatively weakly absorbing carotenoid chromophores [28], and the methodology has not found widespread application.

A further attempt to derive skin carotenoid concentrations has explored skin color saturation measurements [29]. In this method, one of the color tristimulus values, the b^* -value, was measured and compared to the chromaticity diagram of a white reflection standard. Since the b^* -value measures the color saturation from the yellow to the blue region, it can be expected to be influenced by the absorption of skin carotenoids occurring in this spectral range. However, the measurements are influenced not only by the carotenoid absorption but also by the superimposed absorption and scattering effects of blood and melanin, thus leading to rather unspecific results with relatively large errors.

Summarizing the pros and cons of RRS and earlier reflection approaches for the quantitative detection of skin carotenoids, RRS has high specificity and high precision. However it requires excitation with a narrow-bandwidth laser or tightly filtered LEDs, as well as the detection of narrow-bandwidth spectral regions centered on the carotenoid Stokes lines. To compensate for the small Raman scattering cross section, excitation with a relatively high-power light source and detection with a sensitive, high-dynamic range CCD array or photomultiplier detector must be used. As a result the instrumentation is relatively expensive. In contrast, reflection is less specific and less precise due to overlapping chromophores, but the reflected light levels are relatively strong, and the method can be implemented with inexpensive broad-band light sources for excitation and simple filters for detection.

2. Pressure-mediated reflection spectroscopy

In reflection spectroscopy, the diffusively scattered light usually contains spectral regions with diminished light scattering due to the combined absorption of skin chromophores present in the tissue volume near the surface. The shapes and strengths of the prominent absorptions can be easily derived from the reflection spectra if the chromophores are spectrally separated. This is not always the case, however. For the skin carotenoids of interest to us, several potentially confounding chromophores have to be dealt with. Their absorptions are shown schematically in Figure 1, along with the vibronic absorption of β -carotene. They include oxygenated hemoglobin, HbO₂, de-oxygenated hemoglobin, Hb, and to a lesser extent also the absorption tail of flavonoids, FLAV. While HbO₂ and Hb overwhelm the

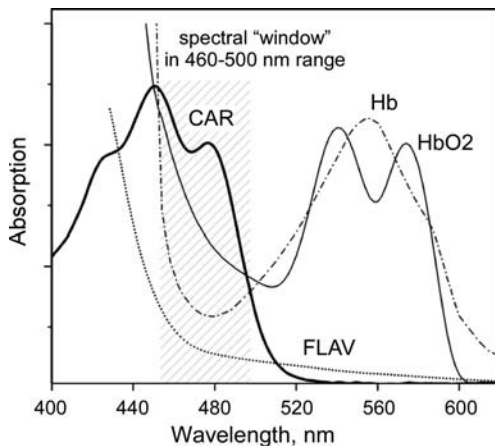


Figure 1 Model absorption spectra of the three main absorbers in melanin-free human skin tissue: oxygenated hemoglobin, HbO₂ (thin solid line), deoxygenated hemoglobin, Hb (thin dash-dotted line), and carotenoids, CAR (shown as an example for beta-carotene as thick solid line). Also shown is the absorption tail of flavonoids, FLAV. A spectral window of relatively small interference for carotenoid detection exists in the 460–500 nm range. See text.

carotenoid absorption in the near UV/blue wavelength region up to about 450 nm, a spectral window of reduced interference exists between about 460 and 500 nm, as sketched in Figure 1. The absorption contribution of flavonoids is relatively small compared to carotenoids in this spectral window. For their independent optical detection a fluorescence approach is feasible [30].

To increase the contrast between the carotenoid absorption strength and the combined absorption background, we apply topical pressure in our reflectivity approach. In this way blood is squeezed out of the measured tissue volume and the resupply is temporarily blocked. As a consequence, overlapping HbO₂ absorptions are effectively removed and any residual HbO₂ is converted into Hb, which has about a factor of 2.5 lower absorption strength in the spectral window relative to HbO₂ (ref. Figure 1).

We tested two reflection-based instrument versions for the pressure-mediated carotenoid measurements, both shown schematically in Figure 2. In one version, spectrally broad “white light” from a tungsten halogen lamp or “white” LED is routed via multimode fiber into a light delivery/collection module, is collimated with a first high-refraction plano-convex lens inside the module, routed through an aperture stop, and imaged onto the skin as a 3 mm diameter excitation disk through a second plano-convex field lens that is in direct contact with the skin. Upon contact, the lens squeezes blood away from the vertex of the lens in radial tissue directions. The detection channel of the module collects light

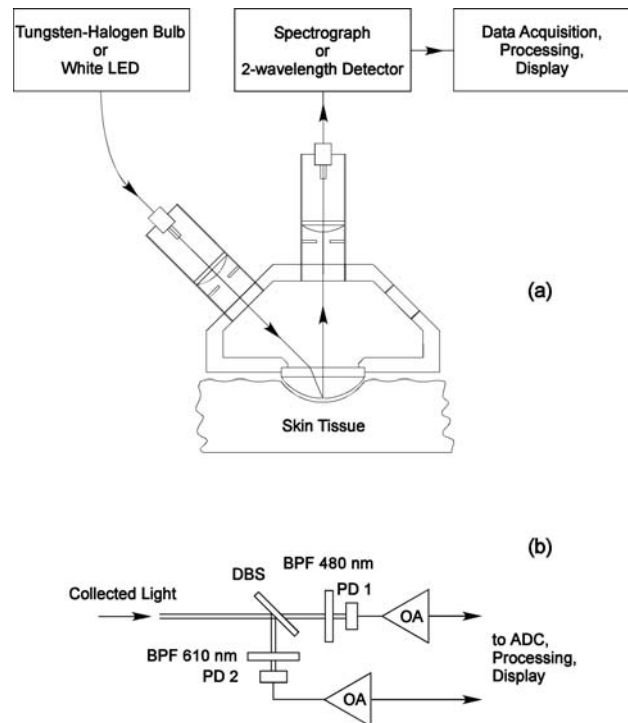


Figure 2 (a) Schematics of skin reflectivity apparatus, consisting of a “white” light source (LED or tungsten halogen lamp), light delivery and collection module that is placed in contact with the tissue site of interest, a spectrograph or two-wavelength detection scheme, and data acquisition, processing and display electronics. The module’s lens is pressed against the tissue site of interest for about 10–15 seconds for skin carotenoid measurements. (b) Details of the two-wavelength photometric instrument variant, in which the detection channel is split via dichroic beam splitter into two separate detection channels, each of which are filtered with band pass filters at 610 and 480 nm, respectively, and further detected, amplified, and processed separately.

that is diffusively reflected from the skin into a 45 degree angle with respect to the direction of the incident light. This geometry ensures that specular reflection of the skin into the detection channel is effectively avoided. Light diffusively reflected into 45 degree direction traverses the contact lens, is apertured, imaged by a lens onto a light collection fiber, and routed into a spectrograph which is coupled to a linear CCD array. The latter is interfaced to a laptop computer for data acquisition, processing, and display. The light source is operated with a current-stabilized power supply that limits current fluctuations to less than 1%. Both fibers have a core diameter of 500 μm. The spectrograph had a resolution of about 7 nm in the visible region.

To monitor and control the topical pressure we use a piezo-resistive load cell that is mounted onto the lens assembly. When pushing the tissue site of

interest against the contact lens, the load cell is pushed against a hard stop. This generates a voltage that is proportional to the applied pressure. The voltage is displayed in real time on the computer monitor and provides visual feedback for the measured subject, who is asked to keep the pressure constant within a pre-selected optimal pressure range of ~ 1 atm $\pm 10\%$.

Prior to skin measurements, a dark spectrum $D(\lambda)$ is recorded that provides a background signal intensity for each pixel of the detector array for data processing, thus allowing one to account for hot pixels of the array as well as minor light scattering inside the optical module and the spectrograph. Also, a diffuse reflection spectrum is measured from a “white” reflection reference standard in the same geometry as the measured skin, and stored in computer memory. For the measurement of dermal carotenoid levels, the contact lens is pressed against the skin tissue site of interest for about 10–15 seconds, followed by the actual measurement, which takes about 2 seconds.

The instrument software calculates the reflectivity spectrum $R(\lambda)$ according to the expression

$$R(\lambda) = \frac{T(\lambda) - D(\lambda)}{S(\lambda) - D(\lambda)} \cdot 100\% \quad (1)$$

where $T(\lambda)$ and $S(\lambda)$ are the intensities measured at wavelength λ from skin tissue and reflectivity standard, respectively, and $D(\lambda)$ is the signal dark spectrum intensity. Subsequently, the program converts the reflectivity spectrum $R(\lambda)$ into an “apparent” optical density spectrum $A(\lambda)$ by taking the common logarithm for each spectral data point of the reflectivity spectrum, using the relation

$$A(\lambda) = -\lg\left(\frac{R(\lambda)}{100}\right) \quad (2)$$

During skin measurements, reflection spectra are acquired, processed into apparent absorption spectra, and displayed in near real-time on the computer monitor, which is updated every second.

In a particularly simple instrument version, the spectrograph is replaced with a photometric two-wavelength detection scheme, sketched at the bottom of Figure 2. The collected light is split into two channels via dichroic beam splitter, filtered with 610 and 480 nm band pass filters, respectively, detected with simple photodiodes, and amplified. Computer interfacing is used again for data processing and display.

Prior to measurements with living tissue we tested our reflection setup with excised human heel skin samples, which like the palm of the hand are bloodless, free of melanin, and contain a relatively thick stratum corneum layer. They are well suited for validation purposes of carotenoid detection methodologies [18]. We first measured the tissue ca-

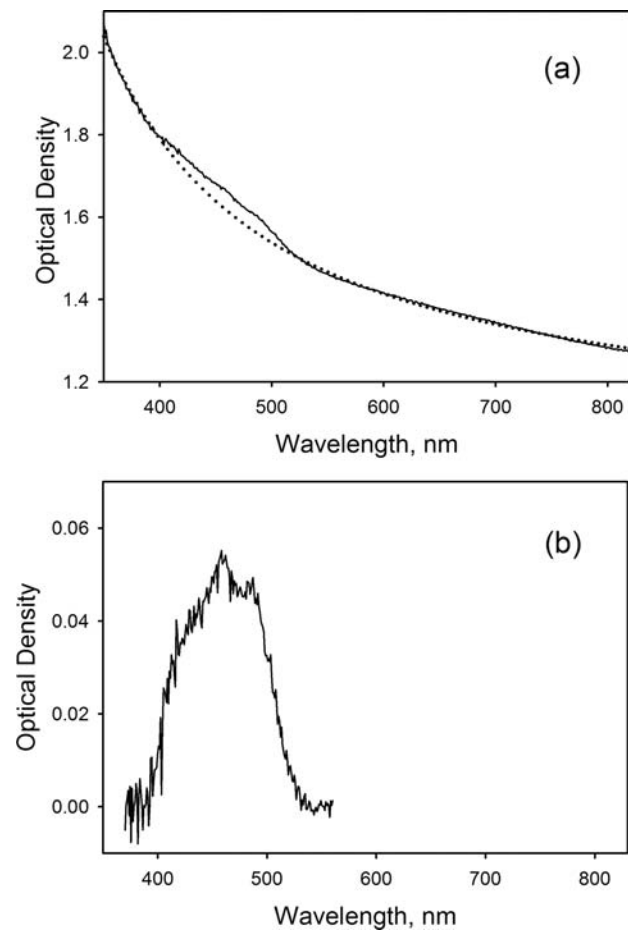


Figure 3 (a) Absorption spectrum (solid line) of excised, bloodless, heel skin tissue sample and associated scattering background (dotted curve). Thickness: 0.7 mm. (b) Absorption spectrum obtained after subtraction of scattering background, revealing all characteristic carotenoid absorption features, including vibronic substructure.

rotenoid absorption directly via transmission measurements, using a conventional UV/VIS/NIR spectrometer (Perkin Elmer). The results are shown in Figure 3, where the upper panel shows the measured tissue absorption as solid line, and the scattering background as dotted line. Subtraction of the two spectra results in the absorption spectrum displayed in the lower panel, which clearly reveals the presence and concentration of carotenoids through their characteristic absorption features. It even reveals the molecules’ three vibronic sub-bands at ~ 430 , 450, and 480 nm, respectively, despite the light having to propagate through the rather strongly scattering tissue material of 0.7 mm thickness. The measured absorption level in this particular sample corresponds to a carotenoid concentration of approximately $2.75 \mu\text{g}$ per gram tissue, which is comparable to HPLC derived results [18].

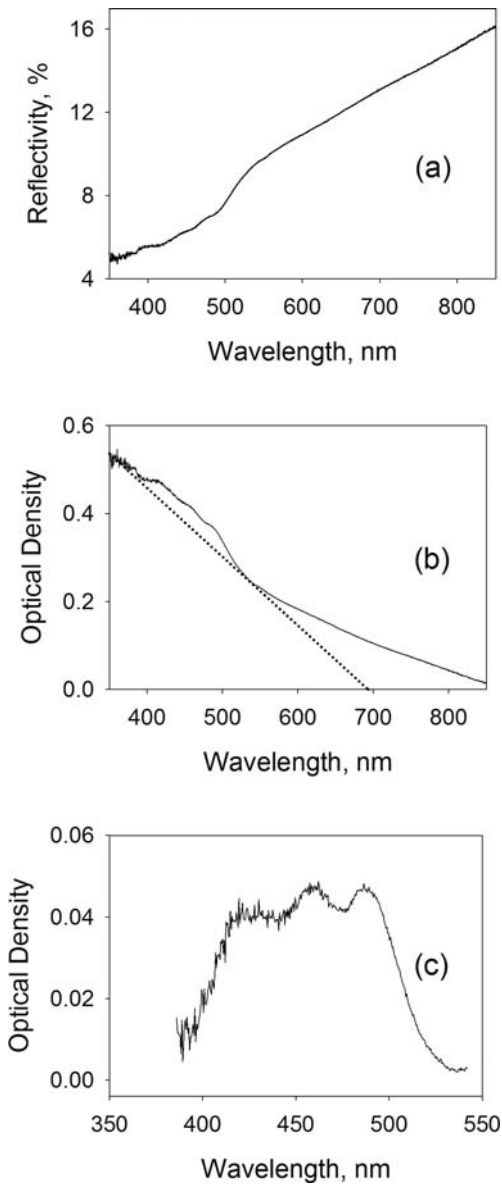


Figure 4 (a) Normalized reflectivity spectrum, (b) derived apparent absorbance spectrum with scattering background, and (c) difference spectrum to background measured with setup of Figure 2, shown for wavelength range 380–540 nm.

Next we measured the reflectivity of the same sample with the spectrograph setup of Figure 2 over the wavelength range 380–850 nm. Plotted in Figure 4, these results show a skin reflectivity that increases gradually from short to long wavelengths (upper panel), with an apparent dip in the 400–530 nm carotenoid absorption range. Plotting the corresponding absorbance spectrum derived with the relation $A = -\lg(R/100)$ for each spectral data point (middle panel), we obtain the carotenoid absorbance again (lower panel) after subtracting the

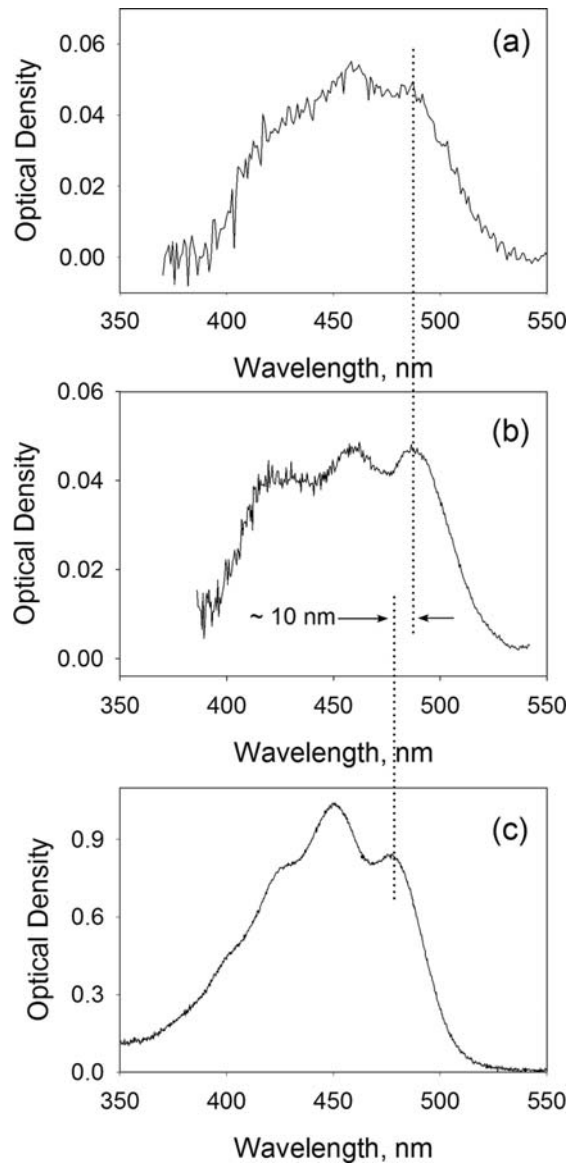


Figure 5 Comparisons of carotenoid absorption features in excised heel skin tissue derived from transmission (a) and reflection (b) measurements, respectively, with absorption spectrum of β -carotene solution in methanol (c). A close resemblance of the skin carotenoid spectra with the absorbance spectrum of the pure carotenoid solution is apparent, again, including spectral positions, halfwidths, and vibronic substructures. In the tissue, the vibronic peaks are shifted by ~ 10 nm to longer wavelengths, as indicated by the vertical dashed lines.

approximated linear scattering background in the 380–530 nm range. The reflectivity-derived absorbance level of 0.04 is roughly the same as the previously derived level via direct transmission measurement (ref. Figure 3).

In Figure 5 we compare absorption- and reflection-derived spectral shapes with the absorption fea-

tures of a pure β -carotene solution in methanol. Importantly, a small, but clearly noticeable ~ 10 nm red shift exists as a consequence of the tissue matrix environment. Furthermore, the reflection-derived absorbance spectrum shows less scattering compared to the absorbance derived-spectral shape, as evidenced by the higher vibronic sub-band modulation in the reflection case, particularly the clearly resolved one-phonon vibronic transition at ~ 480 nm. These results demonstrate the capability of reflection spectroscopy to derive, even in the presence of the highly scattering skin matrix, all spectral absorption characteristics of skin carotenoids such as peak wavelength, half width, and vibronic substructure. The remaining question is whether and to which extent some or all of the carotenoid spectral features can still be differentiated from other chromophores when measuring more conveniently accessible exposed living tissue sites such as the palm of the hand, fingers, etc. In any case, a spectral region of relatively high specificity for the presence of carotenoids

is the vicinity near 480 nm since it retains its sub-band modulation in the presence of the tissue matrix.

In Figure 6, we show reflectivity and corresponding absorbance spectra for living human skin of a volunteer subject, in this case for a thumb tissue site opposite the nail, and show the influence of topical pressure on the spectra. The measurements were carried out with the spectrograph setup of Figure 2.

When only gently touching the contact lens (zero pressure) the reflection spectrum is dominated by the two prominent low-energy, overlapping, HbO₂ transitions in the 540–600 nm range, and the high-energy HbO₂ transition centered near 420 nm. In the tell-tale carotenoid spectral region near 480 nm, only a hint of an absorption feature is apparent. After pressing the thumb with moderate pressure ($\sim 3 \times 10^5$ Pa) against the contact lens for about 10–15 seconds, the blood is squeezed out of the measured tissue volume, the HbO₂ absorption has nearly disappeared as a consequence, and the remaining blood has lost its oxygenation, causing residual weak single-band Hb absorptions in spectral vicinities near 560 and 410 nm, respectively. Most importantly, a significant “clearing” due to the removal of blood also occurs in the carotenoid region of interest, such that the vibronic sub-band region near 480 nm becomes partially resolved and sufficiently isolated for quantification.

We obtained very similar spectra and corresponding results also for other tissue sites, such as the palm of the hand or the inner and outer forearm. In each case, the applied pressure was found to significantly reduce the influence of HbO₂ and Hb absorptions on the spectra and thus to improve the absorption contrast for the carotenoid transition in the 460–500 nm spectral window. The relatively thin skin tissue layer of the inner forearm leads to lower carotenoid absorbance and higher influence of blood, however. Similarly, for the outer forearm with its higher melanin content, relatively complex spectra are encountered. To avoid these problems we limited our tissue locations to the melanin-free, thick stratum corneum sites of the palm and fingertip opposite the nail.

To derive the dermal carotenoid absorption strength quantitatively from the measured reflectivity spectra, we tested several empirical algorithms. In one of the approaches, we subtract from the measured absorption spectrum in the 467–515 nm carotenoid vibronic sub-band region a straight line that connects the spectral points 467 and 515 nm, as illustrated in Figure 7. The rationale is that the amplitude of the resulting bell shaped curve (or alternatively, the enclosed shaded area) is very similar to the spectral features of the vibronic one-phonon absorption region of pure β -carotene (as shown in the insert of Figure 7) and therefore can be assumed to be proportional to the dermal carotenoid concentra-

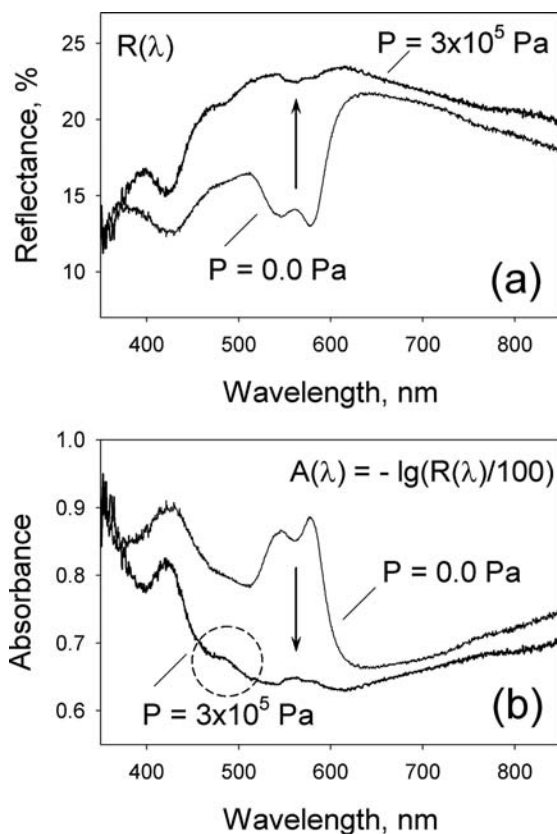


Figure 6 Reflectivity spectra (a) and corresponding absorbance spectra (b) of human skin tissues obtained with the instrument's contact lens touching the skin tissue site with zero pressure and applied pressure of $\sim 3 \times 10^5$ Pa, respectively. A desired optical “blood clearing” effect is achieved in the tissue site for carotenoid measurements with minimal interference from HbO₂.

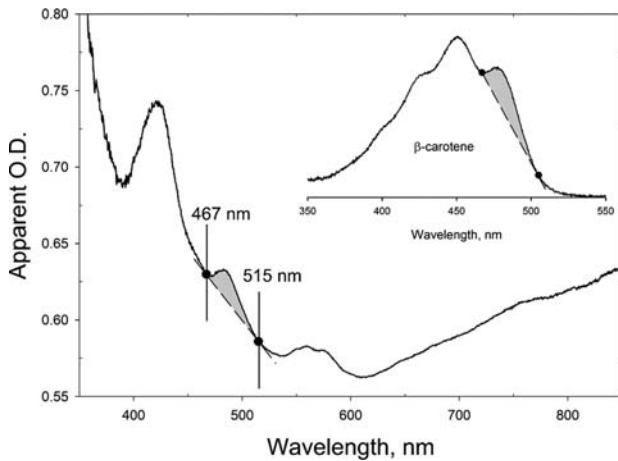


Figure 7 Approximation of carotenoid levels from measured absorption spectra, based on the strength of the carotenoid absorption in the vibronic one-photon transition range between 467 and 515 nm relative to a straight line connection between the two spectral points. The dermal carotenoid absorption spectrum, shown as shaded area, is very similar in this wavelength region to the corresponding absorption of β -carotene in solution (see insert).

tion. The degree of proportionality can be expected to be influenced by the slight broadening of the vibronic transition due to tissue matrix effects as well as the presence of dermal carotenoids with slightly shifted absorption transitions.

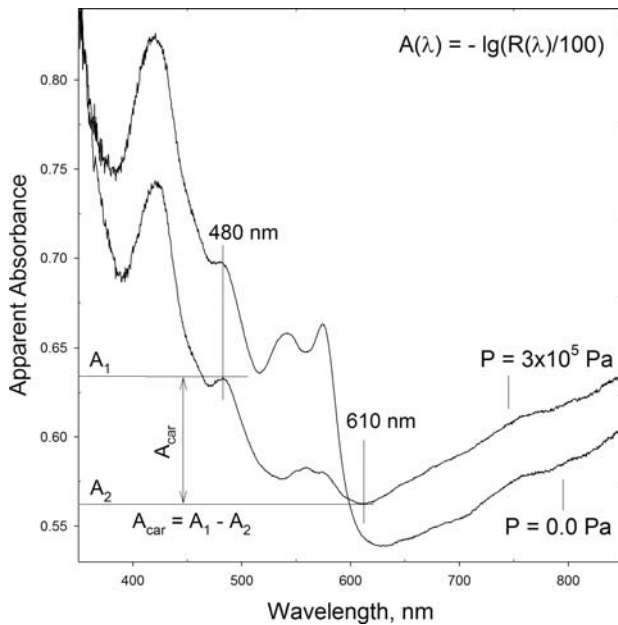


Figure 8 Reflectivity-derived skin absorbance spectra, with illustration of simple alternative data processing algorithm. The apparent absorbance of the carotenoids in the tissue site is chosen as the difference between the total apparent absorbance at 480 and 610 nm after pressure-mediated reduction of HbO₂. See text.

An alternative, even simpler algorithm is based on the difference between the absorbance at 480 nm and the absorbance at 610 nm, thus disregarding the background tissue absorbance in the carotenoid region of interest, as sketched in Figure 8. The carotenoid optical density value derived for the skin tissue in this particular case is $A(480) - A(610) = 0.63 - 0.56 = 0.07$ optical density units. This approach can be rationalized by assuming that under the described pressure conditions, the scattering background at 480 nm is comparable to the background at 610 nm, that any scattering contributions from the skin matrix will be very similar between subjects, and that they will of course be constant for longitudinal studies, i.e. tracking of carotenoid changes upon dietary modifications.

To further illustrate the tissue “clearing” effect, the apparent optical density of skin carotenoids was measured for a volunteer subject at several dozen discrete time points after the subject’s finger was pressed against the probe head lens. The results are shown in Figure 9. For the first 5 seconds, the finger was only in gentle contact with the probe head window and therefore no pressure was applied. In this tissue condition, an artificially high apparent optical density is derived from the reflectivity measurements. When starting to press the finger against the contact lens, the derived optical density values decrease quickly, within a few seconds, by a factor of ~ 2.5 , and then decrease further to a final steady-state level after about 10–15 seconds. The instrument software takes this relatively fast blood clearing effect into account by recording the apparent skin carotenoid absorption level only after a steady state level is reached where subsequent absorbance changes remain within a preset variation range.

It should be noted that the pressure-mediated blood clearing in our reflection approach for the

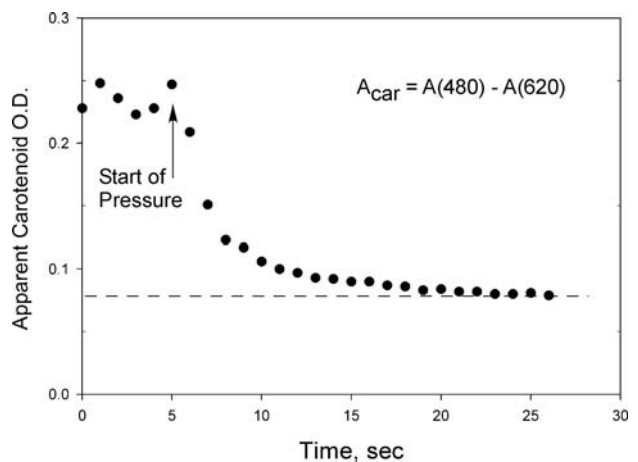


Figure 9 Apparent skin carotenoid optical density versus time during application of topical pressure to the measured tissue site.

measurements of tissue carotenoid levels is much easier to accomplish than the tight control of a constant, reproducible, volume of blood, required when optically measuring blood analytes through the skin. An example is the NIR-Raman-based measurement of blood glucose concentrations in finger capillaries [31, 32]. The measured blood volume and hence the derived optical response in this case is highly sensitive to the pressure exerted on the superficial skin tissue layers, which has to be kept at a relatively low level ($\sim 50 \text{ g/cm}^2$) in order to not squeeze the blood out of the measurement volume. Also, the response is highly sensitive to the precise tissue location of the laser excitation disk, which typically has micron-scale diameter. To control these effects, free space coupling of the laser into the tissue through an open aperture is used in combination with scanning of the laser excitation disk across the ridges of the finger to generate a spatial modulation of the optical response. This modulation is then used to derive the relative contributions of tissue and glucose components, and eventually the glucose concentration [33].

In contrast, reflection-based measurements of skin carotenoid levels require only brief squeezing of blood out of the measured stationary tissue volume in order to remove the blood absorption in the blue-green spectral region. This is achieved by simply pushing the measured skin tissue site with comparatively large pressure ($\sim 1000 \text{ g/cm}^2$) against the convex contact lens of the instrument, which squeezes the blood out radially from its center. Also, the light excitation disk is large ($\sim 3 \text{ mm}$ dia.) in comparison and therefore automatically integrates over small tissue inhomogeneities of the static tissue (ridges, sweat glands, etc.), and the method can be used more generally also with other skin tissue sites

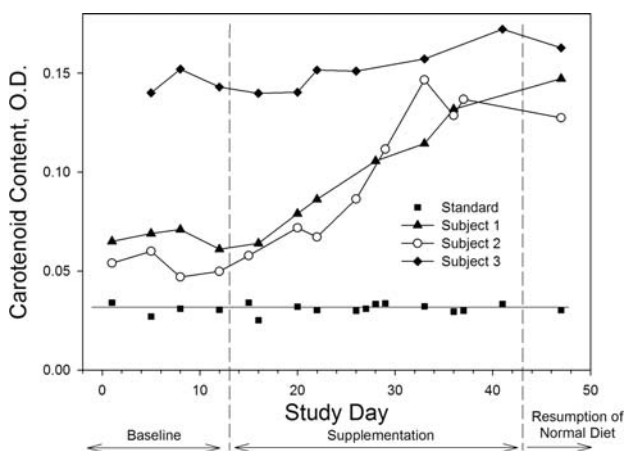


Figure 10 Changes in reflection-derived skin carotenoid levels over time as a response to dietary carotenoid supplementation, measured for three subjects with different respective carotenoid starting levels.

besides fingers, such as the palm of the hand, arm, heel skin, etc.

We tested the usefulness of our reflection methodology for the detection of skin carotenoid uptake upon dietary supplementation. In one experiment, three volunteer subjects consumed two three-ounce servings of carrot juice per day. Reflection-based skin carotenoid levels were measured roughly twice a week with the spectrograph based setup of Figure 2. The results for the apparent skin carotenoid optical density of a thumb tissue site for each subject are shown in Figure 10 for an initial baseline phase of 10 days, i.e. no consumption of juice, and a subsequent supplementation phase of 30 days. During the baseline phase the levels stayed constant within about 10%. Upon supplementation the levels quickly increased for two of the subjects who started with relatively low carotenoid levels, doubled within about 3 weeks, and started to saturate afterwards. The subject with already high skin carotenoid levels at the start revealed only a modest increase over the supplementation phase.

In a separate uptake study, 90 volunteer participants were separated into four groups, with three groups consuming two-ounce servings of β -carotene-containing juices twice daily over a period of 7 weeks (total daily carotenoid amount of 9 mg), and one control group continuing with an un-supplemented regular diet. The participants were directed to drink the juices in combination with regular meals to

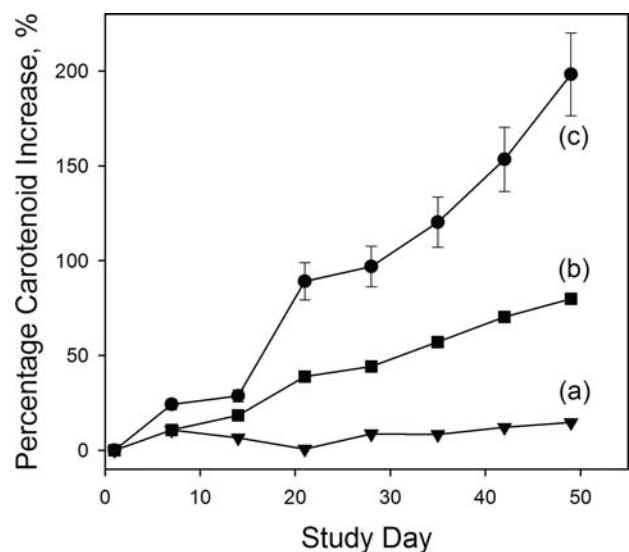


Figure 11 Carotenoid uptake study results for 43 volunteer subjects measured over a period of seven weeks with the 2-wavelength photometric instrument version. (a) average percentage changes of control group (20 subjects) consuming un-supplemented regular diet; (b) average percentage increases of 23 subjects consuming carotenoid containing juice; (c) percentage increases of subject with highest uptake response.

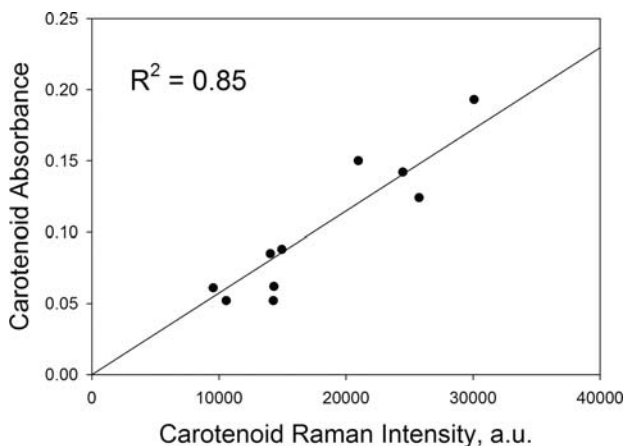


Figure 12 Correlation between reflectivity- and Raman-derived skin carotenoid levels, measured with both methods for 10 volunteer subjects. A high correlation with a squared correlation coefficient of $R^2 = 0.85$ is obtained.

insure adequate fat consumption for optimal carotenoid uptake. All participants were measured once a week with the photometric reflection setup of Figure 2. In each case, three readings were averaged to determine the weekly carotenoid score. Typically, each of the three scores was within 10% of the others. Relevant outcomes of the study are plotted in Figure 11, showing a 200% increase for the subject with the highest response, an approximately 80% increase when averaged over all group participants, and essentially unchanged carotenoid levels for the control group. Further uptake studies are in progress aimed at developing further optimized supplement formulations.

It is interesting to compare the described reflection methodology with our previously developed, completely independent Raman methodology. For this purpose we measured 10 volunteer subjects with both methods. The results are shown in Figure 12, which plots for each subject the reflection derived carotenoid absorbance versus intensities of the carbon-carbon double bond carotenoid Raman response. A high correlation with a squared correlation coefficient of $R^2 = 0.85$ is obtained for the two methods.

3. Discussion

Pressure-mediated reflection spectroscopy is well suited to rapidly measure dermal carotenoid levels with sufficiently high accuracy to allow for comparisons of inter-subject levels as well as to track individual levels in longitudinal supplementation studies. Topical pressure applied to the measured tissue volume in combi-

nation with the described data reduction algorithms significantly improves the method relative to prior implementations. A high correlation with the previously validated RRS method can be regarded as very satisfactory at this stage. Since the RRS method has its own approximations, however, and since is not as accurate as HPLC, the reflection method needs to be separately validated in future studies, comparing the optical results with HPLC-derived carotenoid concentrations of excised tissue samples.

Compared to RRS, the reflection method lacks the high molecule specificity for carotenoid detection considering the absence of a spectrally narrow optical response. However, with proper control of skin absorption conditions and data reduction algorithms, it provides an accurate alternative for the assessment of total dermal carotenoid content and hence as a biomarker for fruit and vegetable intake [17]. An advantage is the simple instrumentation of the reflection approach since it requires only inexpensive incoherent excitation light sources and since it can be carried out with low-spectral-resolution detection schemes.

The insensitivity of the reflection method to the particular composition of dermal carotenoids present in the measured tissue volume can be regarded as an advantage over RRS. Different carotenoid species with differing lengths of the conjugated carbon backbone, such as beta carotene and lycopene, e.g., have slightly shifted spectral absorption bands. Due to the resonantly enhanced Raman scattering cross sections, RRS favors that particular carotenoid species which presents the highest absorption to the used excitation wavelength. However, since the relative skin concentrations of beta carotene and lycopene are not known a priori, and since they can differ significantly between individuals [34], the RRS responses under single monochromatic excitation conditions may not reflect the true composite dermal carotenoid concentration if this wavelength dependence is not taken into account [34].

Also, RRS may underestimate the dermal carotenoid concentrations to some degree since the high autofluorescence background encountered in the method can be seen as evidence for the existence of other chromophores absorbing in addition to the carotenoids at both the excitation and excitation wavelengths, and since the carotenoid RRS response itself shows a saturation effect at high carotenoid concentrations [15]. More importantly, RRS is an absolute detection technique, i.e. the signal strength changes with excitation light intensity and detection sensitivity. It is therefore susceptible to intensity fluctuations and requires an external calibration standard for accurate measurements. In contrast, the reflection method is a relative method. It derives the optical density of dermal carotenoid levels via measurements against a reference spectrum or reference wavelength. Intensity variations therefore cancel out

during the measurements and data processing routines.

In conclusion, the pressure mediated reflection method holds promise as a simple, rapid, and robust optical alternative to RRS for dermal carotenoid measurements. Relative to RRS, the signals are inherently stronger, it is a faster method, calibration procedures with external carotenoid standards are not needed, and the method therefore should be very attractive for widespread applications in the Nutritional Supplement industry, in Nutrition Research, and in Medicine.

Acknowledgements We would like to acknowledge Devin Young and MonaVie, LLC, South Jordan, Utah, for carrying out and supporting the extended Nutritional Supplement Study.



Igor V. Ermakov received a Master's Degree in Physics from the Moscow Engineering Physics Institute in 1993, and a Ph.D. in Laser Physics from the General Physics Institute of the Russian Academy of Sciences in 1997. Later in 1997, he joined the Department of Physics at the University of Utah,

where he has since been active in Biomedical Optics research. His major focus is the development of non-invasive detection methods for carotenoids and related antioxidant compounds in the human retina and skin. In collaboration with medical researchers in the fields of Ophthalmology, Neonatology, Epidemiology and Nutrition Sciences he is investigating the health effects of antioxidants in living human tissue.



Werner Gellermann received his Ph.D. in Physics at the University of Utah, Salt Lake City in 1981, where he currently holds appointments as Research Professor in the Department of Physics and Adjunct Professor at the School of Medicine's Moran Eye Center. Dr. Gellermann's research background is in Solid State Physics, where he developed ionic crystals for novel, wavelength-tunable continuous-wave and femtosecond laser operation in the infrared

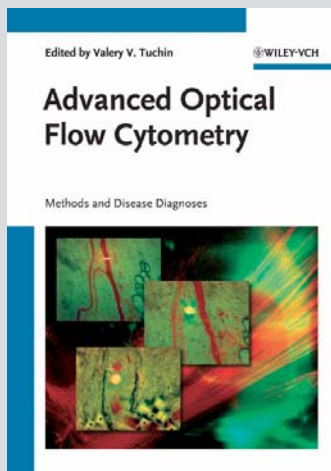
spectral region. In the mid 90's, he and his research group switched to the field of Biomedical Optics, applying their experience with lasers and spectroscopy techniques to the development and commercialization of novel non-invasive detection methods for carotenoid antioxidants and related compounds in living human tissue.

References

- [1] D. S. Michaud, D. D. Feskanich, E. B. Rimm, G. A. Colditz, F. E. Speizer, W. C. Willett, and E. Giovannucci, *Am. J. Clin. Nutr.* **92**, 990–997 (2000).
- [2] L. N. Kolonel, J. H. Hankin, A. S. Whittemore, A. H. Wu, R. P. Gallagher, L. R. Wilkens, E. M. John, G. R. Howe, D. M. Dreon, D. W. West, and R. S. Paffenbarger Jr., *Cancer Epidemiol. Biomarkers Prev.* **9**, 795–804 (2000).
- [3] S. Liu, J. E. Manson, I. M. Lee, S. R. Cole, C. H. Hennekens, W. C. Willett, and J. E. Buring, *Am. J. Clin. Nutr.* **72**, 922–928 (2000).
- [4] Age-Related Eye Disease Study Group, *ARES Rep. No. 22, Arch. Ophthalmol. (Chicago)* **125**, 1225–1232 (2007).
- [5] J. T. Landrum, R. A. Bone, and M. D. Kilburn, *Adv. Pharmacol.* **38**, 537–556 (1997).
- [6] W. Gellermann, R. W. McClane, N. B. Katz, and P. S. Bernstein, U.S. Patent 6,205,354 (March 2001).
- [7] W. Gellermann, I. V. Ermakov, M. R. Ermakova, R. W. McClane, D.-Y. Zhao, and P. S. Bernstein, *J. Opt. Soc. Am. A* **19**, 1172–1186 (2002).
- [8] I. V. Ermakov, M. R. Ermakova, R. W. McClane, W. Gellermann, *Opt. Lett.* **26**, 1179–1181 (2001).
- [9] T. R. Hata, T. A. Scholz, I. V. Ermakov, R. W. McClane, F. Khachik, W. Gellermann, and L. K. Pershing, *J. Invest. Dermatol.* **115**, 441–448 (2000).
- [10] I. V. Ermakov, M. Sharifzadeh, P. S. Bernstein, and W. Gellermann, in: *Carotenoids – Physical, Chemical and Biological Functions and Properties*, J. T. Landrum (ed.) (CRC Press, Atlanta, GA, 2009).
- [11] Y. Koyama, I. Takatsuka, M. Nakata, and M. Tasumi, *J. Raman Spectrosc.* **19**, 37–49 (1988).
- [12] I. V. Ermakov, M. R. Ermakova, and W. Gellermann, *Appl. Spectrosc.* **59**, 861–867 (2005).
- [13] M. Sharifzadeh, D.-Y. Zhou, P. S. Bernstein, and W. Gellermann, *J. Opt. Soc. Am., JOS A* **25**, 947–957 (2008).
- [14] S. D. Bergeson, J. B. Peatross, N. J. Eyring, J. F. Fralick, D. N. Stevenson, and S. B. Ferguson, *J. Biomed. Optics* **13**, 044026 (2008).
- [15] I. V. Ermakov, M. Sharifzadeh, M. R. Ermakova, and W. Gellermann, *J. Biomed. Opt.* **10**, 064028-1–18 (2005).
- [16] W. Gellermann, J. A. Zidichouski, C. R. Smidt, and P. S. Bernstein, in *Carotenoids and Retinoids: Molecular Aspects and Health Issues*, L. Packer, K. Kraemer, U. Obermuller-Jervic, and H. Sies (eds.) (AOCS Press, Champaign, Illinois, 2005), Chapter 6, pp. 86–114.

- [17] S. T. Mayne, B. Cartmel, S. Scarmo, H. Lin, D. Leffel, E. Welch, I. V. Ermakov, P. Bohsala, P. S. Bernstein, and W. Gellermann, *Am. J. Clin. Nutr.* **92**, 794–800 (2010).
- [18] I. V. Ermakov and W. Gellermann, *Arch. Biochem. Biophys.* **504**, 40–49 (2010).
- [19] S. Rerksuppaphol and L. Rerksuppaphol, *J. Med. Assoc. Thai.* **89**, 1206–1212 (2006).
- [20] Y. Shao, J. Qu, and Y. He, *Proc. SPIE-OSA, Biomedical Optics* **6628**, 662817 (2007).
- [21] J. Fluhr, P. Caspers, J. A. van der Pol, H. Richter, W. Sterry, J. Lademann, and M. Darvin, *J. Biomed. Opt.* **16**(3), 035002-1–035002-7 (2011).
- [22] B. B. Betz, J. Diaz, T. A. Ring, M. Wade, K. Kennington, D. M. Burnett, R. McClane, and F. A. Fitzpatrick, *Cancer Prev. Res.* **3**(4), 529–538 (2010).
- [23] P. S. Bernstein, M. Sharifzadeh, A. Liu, I. Ermakov, K. Nelson, X. Shen, C. Panish, B. Carlstrom, R. O. Hoffman, and W. Gellermann, Association for Research of Vision and Ophthalmology (ARVO), Fort Lauderdale, FL, 2012.
- [24] I. V. Ermakov and W. Gellermann, U.S. Patent Office Pub. No. US 2009/0306521.
- [25] J. van de Kraats, D. van Norren, and T. J. M. Berendschot, U.S. Patent Office Pub. No. US 2007/0252950.
- [26] W. Stahl, U. Heinrich, H. Jungmann, J. von Laar, M. Schietzel, H. Sies, and H. Tronnier, *J. Nutr.* **128**, 903 (1998).
- [27] W. Stahl, U. Heinrich, H. Jungmann, H. Tronnier, and H. Sies, *Meth. Enzymol.* **319**, 494–502 (2000).
- [28] F. Niedorf, H. Jungmann, and M. Kietzmann, *Med. Phys.* **32**, 1297–1307 (2005).
- [29] S. Alaluf, U. Heinrich, W. Stahl, H. Tronnier, and S. Wiseman, *J. Nutr.* **132**, 399–403 (2002).
- [30] M. Sharifzadeh, I. V. Ermakov, and W. Gellermann, U.S. Patent Office Pub. No. 2010/0179435.
- [31] J. Chaiken, W. Finney, P. E. Knudsen, R. S. Weinstock, M. Khan, R. J. Bussjager, D. Hagrman, P. Hagrman, Y. Zhao, Ch. M. Peterson, and K. Peterson, *J. Biomed. Opt.* **10**(3), 031111-1–031111-12 (2005).
- [32] J. Chaiken and J. Goodisman, *J. Biomed. Opt.* **15**(3), 03007-1–03007-15 (2010).
- [33] J. Chaiken, B. Deng, R. J. Bussjager, G. Shaheen, D. Rice, D. Stehlik, and J. Fayos, *Rev. Sci. Instr.* **81**, 034301-1–034301-11 (2010).
- [34] I. V. Ermakov, M. R. Ermakova, J. Lademann, and W. Gellermann, *J. Biomed. Opt.* **9**, 332–338 (2004).

+++ Suggested Reading +++ Suggested Reading +++ Suggested Reading +++



2011. XXXVIII, 702 pages,
302 figures. Hardcover.
ISBN: 978-3-527-40934-1

Edited by VALERY V. TUCHIN
Saratov State University, Russia

Advanced Optical Flow Cytometry

Methods and Disease Diagnoses

A detailed look at the latest research in non-invasive in vivo cytometry and its applications, with particular emphasis on novel biophotonic methods, disease diagnosis, and monitoring of disease treatment at single cell level in stationary and flow conditions.

This book thus covers the spectrum ranging from fundamental interactions between light, cells, vascular tissue, and cell labeling particles, to strategies and

opportunities for preclinical and clinical research. General topics include light scattering by cells, fast video microscopy, polarization, laser-scanning, fluorescence, Raman, multiphoton, photothermal, and photoacoustic methods for cellular diagnostics and monitoring of disease treatment in living organisms. Discussions of advanced methods and techniques of classical flow cytometry are also presented.

Register now for the free
WILEY-VCH Newsletter!
www.wiley-vch.de/home/pas

WILEY-VCH • P.O. Box 10 11 61 • 69451 Weinheim, Germany
Fax: +49 (0) 62 01 - 60 61 84
e-mail: service@wiley-vch.de • <http://www.wiley-vch.de>

 **WILEY-VCH**